Quantifying the Long-Term Impact of Electric Vehicles on the Generation Portfolio

Aonghus Shortt, *Student Member, IEEE*, and Mark O'Malley, *Fellow, IEEE*

***Abstract*—Electric Vehicles (EVs) charged in a manner that is optimal to the power system will tend to increase the utilization of the lowest cost power generating units on the system, which in turn encourages investment in these preferable forms of generation. Were these gains to be substantial, they could be reflected in future charging tariffs as a means of encouraging EV ownership. However, where the impact of EVs is being quantified, much of the system benefit can only be observed where generator scheduling is performed by unit-commitment based methods. By making use of a rapid, yet robust unit-commitment algorithm, in the context of a capacity expansion procedure, this paper quantifies the impact of EVs for a variety of demand and wind time-series, relative fuel costs and EV penetrations. Typically, the net-cost of EV charging increases with EV penetration and CO_2 cost, and falls with increasing wind. Frequently however these relationships do not apply, where changes in an input often lead to step-changes in the optimal plant mix. The impact of EVs is thus strongly dependent on the dynamics of the underlying generation portfolio.**

***Index Terms*—Electric vehicles, power generation planning, wind power generation.**

Nomenclature

η_{th}	Thermal efficiency (%).
C_{avg}	Average cost (euros/MWh).
C_{CO_2}	CO_2 costs $(\text{euros}/\text{t}_{CO_2})$.
C_{FL}	Full-load cost (euros/h).
C_{fuel}	Gross fuel costs $(\text{euros}/\text{MWh}_{fuel})$.
C_{incr}	Incremental cost (euros/MWh).
C_{NL}	No-load cost (euros/h).
$C_{O\&M}$	O&M Costs (euros/MWh).
C_{start}	Cost of starting unit type.
f_{obj}	Annual costs (objective function).
G	Hourly costs.
I	Installed flexible generation (MW).
N	Number of inflexible generators (*integer*).
P_{dem}	System electrical demand (MW).
P_{max}	Maximum unit production (MW).
P_{min}	Minimum unit production (MW).
P_{res}	Minimum total reserve (MW).
P_{wind}	Available wind production (MW).
$R_{CO_2/\text{MWh}}$	Emissions Ratio $(\text{t}_{CO_2}/\text{MWh}_{fuel})$.
R_{NL}	No load ratio.
$t \in T$	Time-steps.
$u_{fl} \in U_{fl}$	Flexible generation types.
$u_{in} \in U_{in}$	Inflexible unit types.
$u_{all} \in U_{all}$	All generation types.
V_{curt}	Decision variable: Wind curtailment (MW).
V_{gen}	Decision variable: Electrical output (MW).
V_{online}	Decision variable: Number online (*binary*).
V_{start}	Decision variable: Unit start (*binary*).

Manuscript received October 01, 2012; revised February 28, 2013, June 14, 2013, and August 28, 2013; accepted October 12, 2013. Date of publication November 04, 2013; date of current version December 24, 2013. This work was conducted in the Electricity Research Centre, University College Dublin, Ireland, which is supported by the Commission for Energy Regulation, Bord Gáis Energy, Bord na Móna Energy, Cylon Controls, EirGrid, Electric Ireland, Energia, EPRI, ESB International, ESB Networks, Gaelectric, Intel, SSE Renewables, and UTRC. This publication has emanated from research conducted with the financial support of Science Foundation Ireland under Grant Number 06/CP/E005. Paper no. TSG-00662-2012.

The authors are with the School of Electrical, Electronic and Communications Engineering, University College Dublin, Dublin, Ireland (e-mail: aonghus.shortt@ucd.ie; mark.omalley@ucd.ie).

Color versions of one or more of the figures in this paper are available online at http://ieeexplore.ieee.org.

Digital Object Identifier 10.1109/TSG.2013.2286353

I. Introduction

ELECTRIC VEHICLEs (EVs) are increasingly seen as one of the leading vehicle propulsion technologies to replace conventional fossil-fueled combustion engines in the medium to long term. An obvious means of reducing CO_2 emissions, EVs could also have a significant role in improving urban air quality, reducing primary energy waste and diversifying the supply of primary energy in transportation [1]–[3]. However, when compared to conventionally fueled vehicles, the EV user is constrained by the capacity of their battery and the rate at which it can recharge. Larger batteries can remedy these problems to some degree, but at a significant cost. It has been proposed that EVs could potentially offer various benefits to the power system [4], [5]. If these are substantial, then a financial mechanism could be used to pass some portion of the benefit on to EV buyers, in the form of savings on charging[1] or reduced vehicle

[1]Regulatory or legislative changes may be required for electricity retailers to offer reduced prices for specific end-uses.

purchase price. This paper attempts to determine the net-cost of charging EVs from the perspective of the power system, to determine if such a mechanism would have any merit.

With the necessary smart-grid infrastructure, EVs can draw energy from the power system when the net-demand, i.e. demand minus variable generation, is at its lowest. In so doing, the vehicles will make use of the lowest cost power plants. The extra utilization of these baseload plants will also reduce the cost of cycling these units, which is a combination of operating the plants at part-load and engaging in costly shutdowns and startups [6]–[9]. Previous analyses of long-term EV benefits have only been able to consider a subset of these effects [10]–[13]. In these studies the generators have been scheduled via economic dispatch, which in effect aggregates units into blocks of generation and assigns production based on estimates of the average cost of each generation type. Such 'merit order' scheduling over-estimates the utilization of baseload generators [14]. By not considering the unit-commitment (which units are online and offline at each moment), the cost of starting units, and the changes in the schedule owing to start costs, cannot be determined. These problems become increasingly severe with increasing variable renewables [14]. The downside of considering the commitment of generators is a very significant increase in computation time. Generally, these mixed-integer linear programs take orders of magnitude longer to execute, which tends to hamper the scope and granularity of analysis [14], [15]. Unit-Commitment and Economic Dispatch (UCED) models are therefore usually applied in snapshot analyses, where the set of generators is fixed. For example, [16] considers the impact of EVs on the emissions of oxides of sulphur, nitrogen and carbon in the ERCOT system. Their UCED methodology allows for the accurate determination of changes in power system operation and thus emissions and costs, but can only point to potential improvements in the generation mix as a consequence of flexible EV load. Thus one of the main contributions of this paper is in proposing a computationally efficient means of analyzing the long-term impact of EVs, using a methodology that allows for changes in the generation fleet, in response to beneficial changes in the commitment of generation.

Previous work by the authors has quantified the importance of using UCED models [14], by comparing the performance of a mixed-integer optimization model and a linear dispatch model over a large range of input sets. The accuracy of the linear dispatch model was often poor, but the UCED model was encumbered by its computation time. In response to this, a UCED algorithm has been developed which is equivalent in terms of its inputs and outputs to the aforementioned optimization models, but crucially executes in a much shorter length of time. The capacity expansion algorithm and the UCED scheduling algorithm are discussed in more depth in Section II. Section III details the input data and assumptions used. Section IV presents the results and Section V offers some conclusions. Finally, some supplementary description of the scheduling algorithm is given in Appendix A.

II. Methodology

It has been assumed here that EVs are to be charged so as to confer the maximum realisable benefit to the generation on the system. To this end, a vehicle charging algorithm is used to allocate the EV charging energy so as to raise the minimum net-demand in each day to the greatest degree possible, with some limitations on the number of vehicles available for charging at any one time. This controlled charging strategy, often referred to as *valley-filling* [17], will tend to reduce part-loading and start-ups of generation plant. It will also utilize the highest merit (lowest unit-cost) plants and will tend to minimize the need for extra generation capacity where charging must take place near the annual net-demand peak. The charging schedules determined by this method will not necessarily be the minimal cost solution, but will certainly be very close.

Overall then, the extra generation costs from EVs will tend to be somewhat offset by virtue of their flexibility in charging. The tariff for charging vehicles should logically reflect this as the average cost of supplying the EV demand will be less than the average cost of supplying the rest of the demand. In the long-term, investment will be led by expectations of how new plant will operate. Owing to EVs, new plant will be online more often, and whilst online will enjoy reduced starts and increased loading. This will favor higher-merit plants, which tend to be costly to build and are less suitable for cycling, but tend to also have the lowest production costs [9], [18], [19]. Therefore, EVs should have a beneficial impact in the long-term plant mix, which should be accounted for when considering the net-cost of vehicle charging.

The complete long-term impact of EVs is thus reached by determining the change in total fixed and variable system costs due to the addition of EVs, over a sufficiently long period to account for how the power systems adapts in response to presence of the EVs.

A. Capacity Expansion Model

Here a capacity expansion model is used to quantify this change in fixed and variable costs (Fig. 1). The procedure begins by setting up all of the necessary input data. The EV charging demand is added to the net-demand series, as described at the start of this section. The wind time-series is added to this to yield a demand series that includes EV demand. This series along with the wind time-series are later used as inputs into the scheduling model, which itself does not distinguish between EV demand and regular demand. For simplicity the total demand, wind penetration and EV penetration are the same each year. Also, EV and generation technology is assumed to be fixed over the period. Thus, for a given year where a capacity addition is required, the relative merits of the different expansion options are driven by two factors: the units that have retired and the fuel costs over the period those plants will operate over.

Since the demand and wind time-series are different for each system, using the same initial set of generators for each system would be inappropriate. Instead, a total installed capacity is chosen and each combination of available plant types that meets this capacity is determined. Each of these combinations is scheduled using a unit-commitment algorithm and the least cost plant combination is selected. Then, each year, certain existing plants are retired according to a pre-defined retirement schedule (Appendix C) and if the total capacity has reduced such that the capacity margin is less than the initial capacity margin, then an expansion must take place. In an expansion,

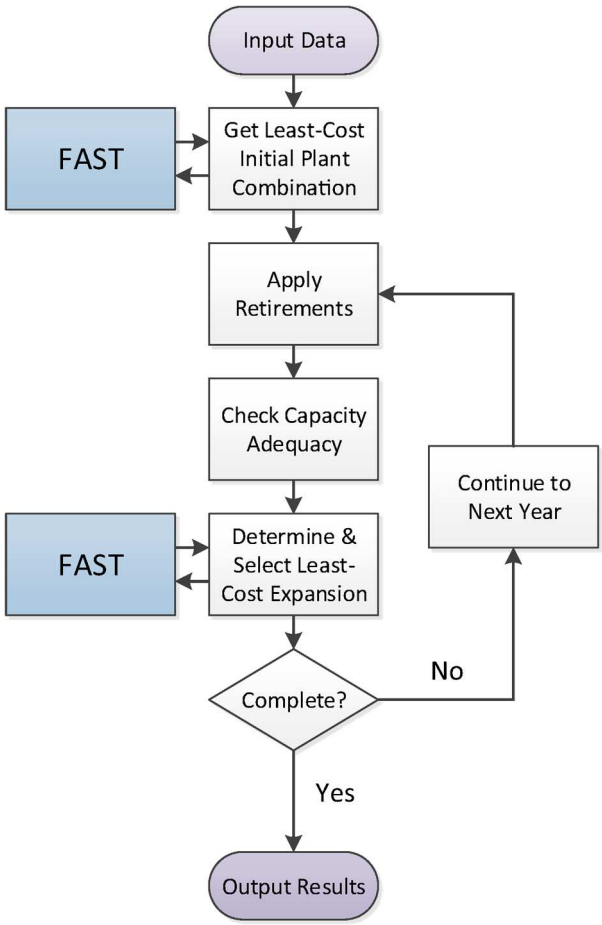

Fig. 1. High-level flow chart broadly outlining the capacity expansion methodology.

the deficit of generation required to have sufficient capacity is determined. Then, the combinations of new plants (and blocks of capacity, in the case of small plants) that would guarantee sufficient capacity without excess whole units, is determined. Each of these sets of new plants is considered by adding them to the existing set of generators, and scheduling the combined set of plants for a period equal to the longest plant-life in the set of new generators. The set of new plants that yields the lowest total system costs is chosen as the optimal expansion. This process of retirement and expansion continues for a set number of years.

B. Unit-Commitment Model

Conventional mixed-integer programming approaches were found to be overly computationally intensive and linear programming models insufficiently accurate [14]. A unit-commitment algorithm, called *FAST*, is used to determine least-cost schedules, as a sub-model to the capacity expansion algorithm.

The FAST algorithm assumes that two broad groups of generation plant can be considered: the first group, the *inflexible plant* types, are subject to some combination of poor-part loading capability, high start costs, high no-load costs and large installed capacity, and so the production costs of these generators are poorly represented by linear variables. Plant types in this group include combined-cycle gas plant and coal-fired steam-cycle plant. The second group, the *flexible plant* types represents those types of plant that have been designed to respond to variability and intermittency and are therefore inexpensive to start and have reasonable part-loading capabilities. Plant types in this group include typical single-cycle gas and distillate plant, which are the types most often used for peaking operation.

The inflexible plant types are defined by a no-load cost (euros/h), an incremental cost (euros/MWh), a start cost and the number of units installed. The flexible plant types are represented by an average cost (euros/MWh) and the capacity that is installed of that type. The flexible plants can thus be arranged in the order in which they will be used, since they only differ in their average costs. The flexible plants are taken as the default producers and the unit-commitment is devised by moving chronologically through the year, determining where starting inflexible units would reduce costs as compared to production from the flexible types. Starting an inflexible unit incurs a start cost, so a start will only occur where the cost of doing so is exceeded by the savings to be made in hourly costs. Also, since there will be multiple inflexible types, it is necessary to start a unit of the inflexible type that would reduce costs to the greatest extent.

An illustration of the algorithm is given in Fig. 2. There is an inner loop and an outer loop. The outer loop, whose progress is tracked by the counter t, progresses forward in time, in search of instances where an inflexible unit start or stop *could* reduce costs.

The inner loops, which considers starts and stops is highlighted in gray in Fig. 2. The logic for starts and stops has been combined to save space and so the figure refers to a commitment *change* to generically refer to a stop or a start.

The inner loop can be entered at decision block A. If the Net-Capacity Demand (NCD) which equals demand minus wind plus spinning reserve, is greater than the quantity of online inflexible capacity (*OnCap*), then an inflexible unit start may reduce costs and *may* be considered. Two additional constraints determine where a start will be considered or not: First, if there are no further units left to start, a start cannot occur. Second, if a unit *stop* has occurred at or after the current time-step, then a start would not be justified until after that time (note: after a start or stop, the algorithm returns to the time-step at which consideration of the relevant commitment change began).

The inner loop can also be entered at decision block B. Here, if *OnCap* (online inflexible capacity) exceeds NCD, then a unit stop may reduce costs and again, may be considered: A unit stop will not be considered if the number of online inflexible units is at the minimum number allowed (for system inertia reasons). And similarly to decision block A, a stop will not be considered if a start has occurred at this time-step or after it.

The first step in the inner loop is to set the inner loop counter ti to equal the outer loop counter t. This way, after a successful commitment change, the inner loop can repeat from the time-step it started at.

Next, a dispatch of the current commitment is performed to determine the *no-change costs*. Then, a unit of each inflexible type is added (in the case of a start) or removed (in the case of a stop) and new dispatches are performed for each removal or addition. The saving from each potential commitment change

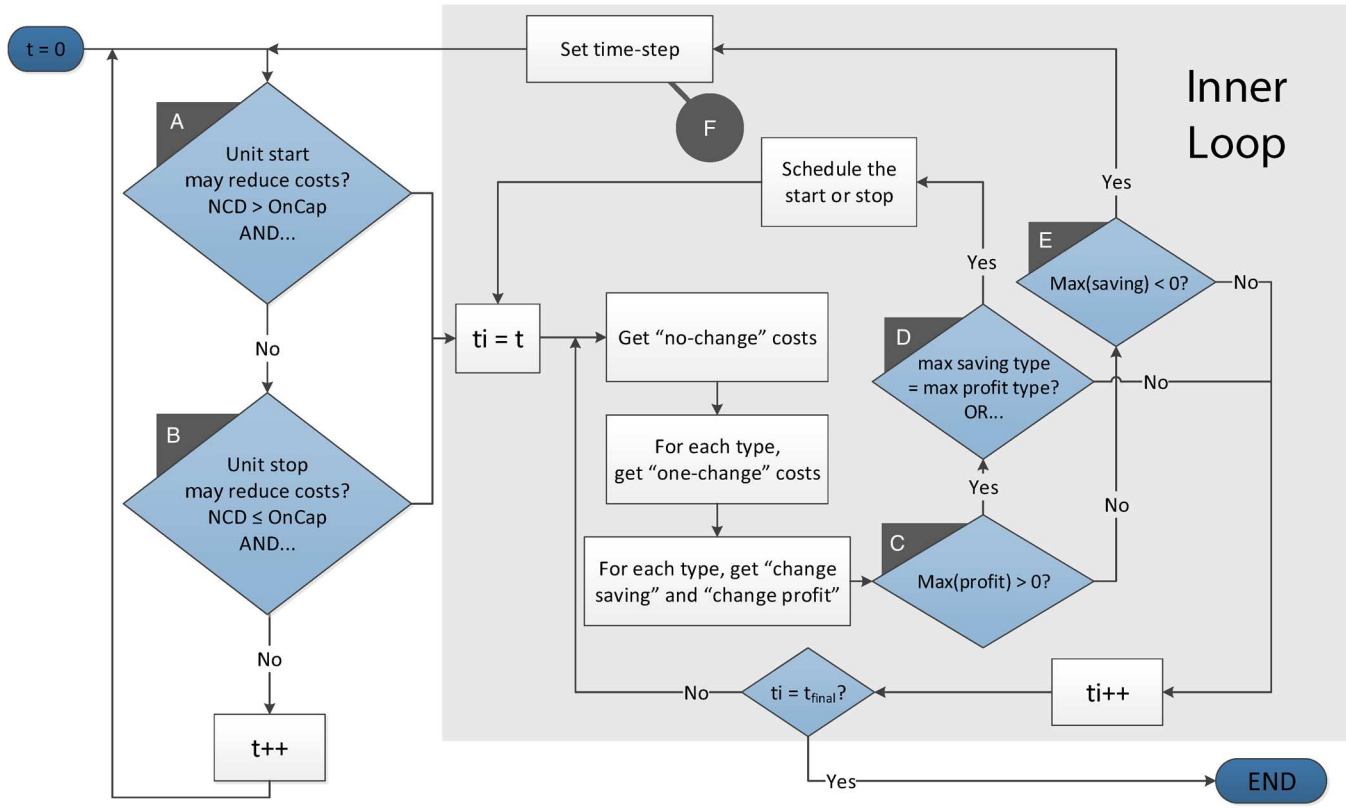

Fig. 2. Logical structure of FAST algorithm, in somewhat simplified form.

is noted (the *change saving*) along with the *change profit*. The change profit for each type equals the change saving for that type minus its start cost. It is the same relation for stops because if a unit stops, it will have to incur a start cost to start again. Thus the cost of starting is effectively the cost of changing between online and offline states: Once the system saving from stopping a unit exceeds the cost of starting it again, then assuming the unit starts again, the unit stop will have yielded an overall cost saving to the system.

Next, decision block C checks to see if the largest *change profit* recorded so far is positive. If this occurs, a commitment change will occur before the inner loop final exits, though in these circumstances it may not happen in this iteration of the inner loop, as a different unit type may yield a higher profit in a future iteration.

If a positive *change profit* has been recorded since the inner loop was entered, execution proceeds to decision block D. Here, a commitment change will occur if the type with the largest *change profit* is also the type with the largest *change saving*. A commitment change will also occur if by this iteration of the inner loop, all types that can make the commitment change now have a negative *change saving*. The justification for making the commitment change once the largest *change saving* type is also the largest *change profit* type is that unit types with a lower start cost will tend to initially have larger a *change profit*. However, there may be unit types with higher start costs and lower hourly costs that would eventually yield a greater *change profit*. Thus, longer duration peaks will tend to be met by higher start cost, lower hourly cost unit types and shorter duration peaks by lower start cost, higher hourly cost types, or by flexible generation types. If a commitment change is made, the inner loop counter is moved back to the position of the outer loop counter and the inner loop repeats to see if further commitment changes should occur. When a commitment change occurs, further commitment changes of the same type are increasingly unlikely as the system will tend towards the ideal level of online capacity. If the conditions for a commitment change are not met at D, the inner loop counter is incremented and assuming the end of the year (t_{final}) has not been reached, the inner loop repeats.

If at decision block C, a positive *change profit* has yet to occur, execution passes to E. If the *change saving* for each applicable type is negative, then the inner loop will exit. Before exiting the outer loop counter t has to be moved forward. If during the consideration of a start, there was an instance of part-loading, i.e. NCD fell below *OnCap*, then t will be moved forward to the time-step at which that occurred, as a unit stop should be considered from that time-step. Likewise during the consideration of a stop, if there was any production by flexible plant, i.e. NCD rose above *OnCap*, then t will be moved forward to the relevant time-step, so that a unit start can be considered from that time-step. If at least one type has a positive *change saving* at E, the inner loop repeats, assuming the end of the year has not been reached.

The algorithm was originally designed to solve a particular mixed integer formulation of the unit-commitment problem and thus the schedules arising from FAST algorithm satisfy all of the MIP constraints. Also, both methods seek to minimize costs, which are defined in the same way in both. Therefore, the perfor-

TABLE I
SUMMARY DATA FOR EACH SYSTEM

Category	ERCOT	Finland	Germany	Ireland	Sweden
Load Factor (demand)	55.2%	68.8%	69.8%	65.6%	62.6%
Capacity Factor (wind)	24.5%	27.8%	15.4%	30.1%	21.1%

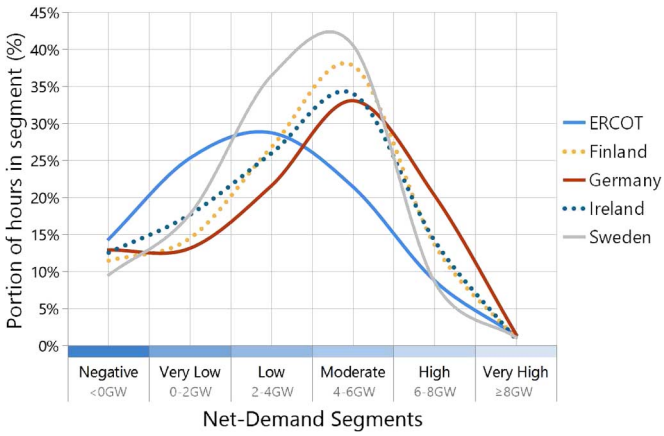

Fig. 3. Net-demand values segmented by magnitude for each system. In each case annual wind output equal to 50% of demand. Curves are interpolations.

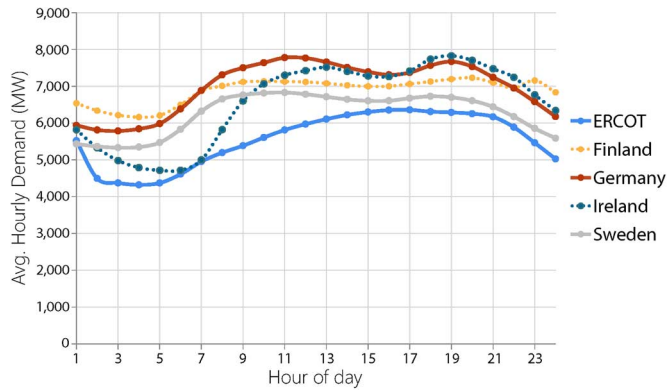

Fig. 4. Average demand by hour of the day (interpolated).

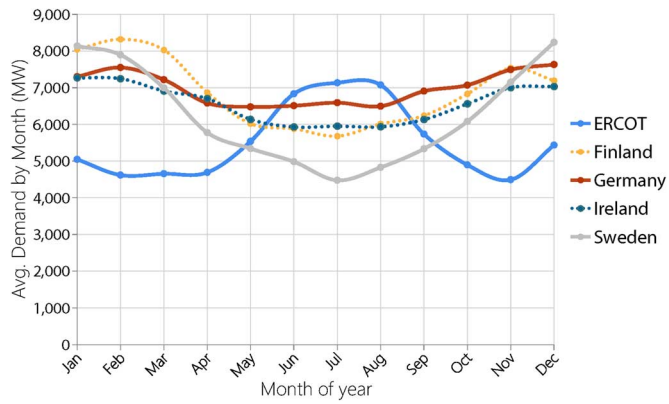

Fig. 5. Average demand by month of year (interpolated).

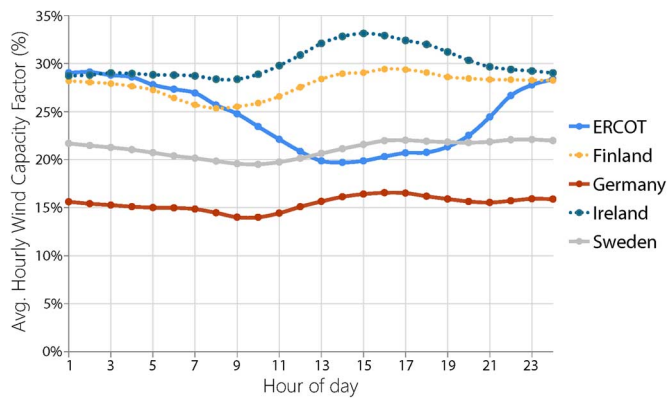

Fig. 6. Average wind capacity factor by hour of day (interpolated).

mance of the algorithm can be directly compared in terms of the *similarity* between the resulting schedules, the *optimality* of the schedules (where the MIP solver is set to determine schedules to a particular optimality gap) and the *computation time*. The formulation of this equivalent MIP, as well as a performance comparison under these headings can be found in Appendix A.

Neither the algorithm nor its equivalent formulation consider non-spinning reserve, minimum up, down and synchronization times, ramping limits, nor the transmission network.

III. INPUT DATA

Five power systems are considered: the Electric Reliability Council of Texas (ERCOT), Finland, Germany, Ireland and Sweden. For each system, hourly metered demand and wind capacity factors are used. System demand is scaled such that the demand peak is 10 GW in each case, to enable comparison between the results from each system. For each wind case, the wind capacity factor time-series is scaled such that the total wind production in a year is equal to some percentage of the total annual system demand. Where wind power curtailment occurs, the actual wind penetration would be somewhat lower than stated.

Since the wind capacity factor time-series are derived from system-wide wind output data recorded at a particular installed capacity, scaling of the wind capacity factor series to different levels of installed wind will under or over state the level of variability, to at least some degree [20]. This effect has been minimized by selecting wind capacity factor time-series derived from a large number of well-dispersed wind farms.

Table I and Fig. 3 outline the gross characteristics of the demand and wind time-series used. Beyond these gross characteristics, system demand varies on diurnal, weekly and seasonal cycles. Wind production for its part, is often strongly seasonal and also exhibits some diurnality. The coincidence of demand and wind is the least fortuitous in ERCOT, where winds tend to be stronger at night (Fig. 6) and during the winter (Fig. 7), in opposition to the broad demand pattern there (Fig. 4 and Fig. 5). Average demand is much lower than peak demand in ERCOT also, as indicated by its low load factor. Finland and

TABLE II
GENERATION UNIT PARAMETERS

Technology Type		Min. Output *MW*	Max. Output *MW*	Thermal Efficiency %	No Load Ratio	Start Costs *€ per start*	Fixed Costs *€ per MW*	O & M *€ per MWh*	Plant Life *Years*
Inflexible	Coal	200	600	40%	0.06	50,000	115,567	2.8	30
	CCGT	200	400	58%	0.23	100,000	63,851	2.7	20
Flexible	OCGT			30%			34,720	6.2	20
	ADGT			43%			50,411	5.2	20

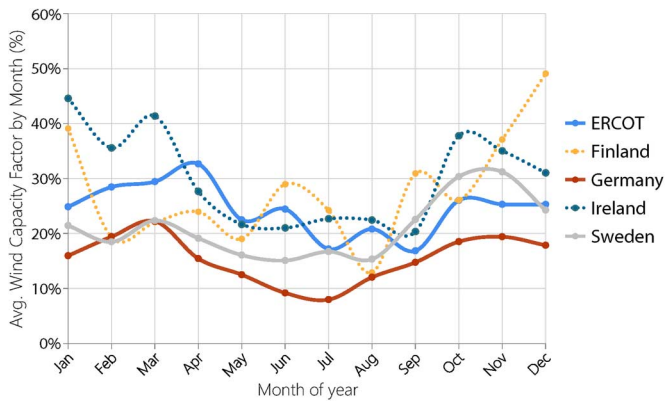

Fig. 7. Average wind capacity factor by month of year (interpolated).

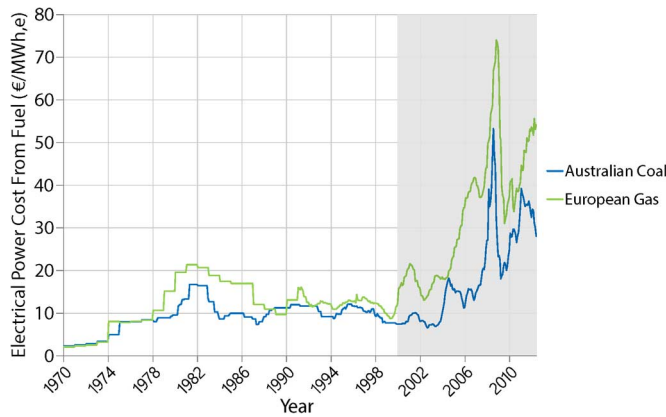

Fig. 8. World Bank historical fuel costs net of full-load thermal efficiencies (CCGT: 58%, Coal: 40%). Shaded region indicates selected range.

Germany have the highest load factors and are both windier during the colder months, but Germany has high diurnal demand variability whereas Finland's demand varies more strongly on a seasonal basis. Ireland demonstrates the highest demand variability, and has a good correlation between demand and wind on a seasonal and diurnal basis. Swedish demand is much greater in winter than summer, but shows the smallest average diurnal range and has the most stable wind output levels by hour of day and by month of the year.

A variety of systems has been used, solely to infer the impact of different demand and wind profiles on the long-term impact of EVs. Thus the systems are represented only by their demand and wind time-series and no consideration is made for the actual generation, storage or transmission assets within the systems or interconnection to neighboring systems. Instead a generic and representative set of plant types has been chosen (Table II), including coal and Combined-Cycle Gas Turbine (CCGT) units, and Open-Cycle Gas Turbine (OCGT) and Aero-Derivative Gas Turbine (ADGT). The initial least-cost set of generators and the generators selected at each stage of the capacity expansion are taken from this set. It should be noted that the initial least-cost generator set does not necessarily reflect the actual generation mix in these systems. Further, the actual generation mix in a system is determined by a complex interaction of policy goals, market environments, available resources and much else.

For the inflexible types, which have varying thermal efficiencies across their output ranges, the listed *Thermal Efficiency* (η_{th}) refers to the thermal efficiency of the generation technology at max output. These units are assumed to have linear production cost curves. The *No Load Ratio* (R_{NL}) indicates the portion of full-load costs (C_{FL}) that is incurred in generating a net-zero level of electrical power, that is, the cost of fuel to overcome windage, friction and to power ancillary equipment (1). The incremental cost, C_{incr} (euros/MWh) can then be calculated as the full-load costs minus the no-load costs, all divided by the maximum plant output, P_{max} (2)

$$C_{FL} = \frac{P_{max}}{\eta_{th}} \cdot (C_{fuel} + C_{O\&M} + C_{CO_2} \cdot R_{CO_2/\mathrm{MWh}}) \quad (1)$$

$$C_{incr} = \frac{C_{FL} - (C_{FL} \cdot R_{NL})}{P_{max}} \quad (2)$$

The price series for thermal coal and natural gas is required to reflect the contemporary volatility in coal and gas prices, and the correlation between them. Fuel price forecasts often do not exhibit these two desired characteristics and are usually proprietary. It has therefore been decided to derive base fuel price time-series from historical values (where the electrical cost from coal tends to be lower) and to use the cost of CO_2 emissions as a proxy for scenarios where the cost of electricity from coal increases relative to gas: CO_2 emissions from coal per unit of electrical power are of course significantly higher for coal than for gas. The required number of annual values has been selected by interpolation from the World Bank monthly fuel-price series from the year 2000 until mid-2012 (Fig. 8) [21]. The same fuel prices are used for each system.

The penetration of EVs is rated in terms of percent of system demand, ranging from 0 to 25% of system demand in steps of 5%. EV penetration given in this way is directly comparable to the wind penetration levels, which are also given as a percentage of system demand, ranging from 0 to 50% in steps of 10%. The EV penetration corresponds to an annual quantity of charging energy. Thus, given the annual electricity demand and the EV penetration, the average daily charging demand for all EVs can be determined (Table III).

TABLE III
ELECTRIC VEHICLE INPUT DATA. EXAMPLE USING SCALED ERCOT DEMAND AND TEXAS TRANSPORT DATA [24]–[26]

Base Electrical Demand	48.4	TWh/year
EV Energy Penetration	5	%
EV Charging Energy	2.42	TWh/year
Daily Total EV Demand	6630	MWh/day
Average Vehicle Travel	20,790	km/year
Vehicle Efficiency	0.2	kWh/km
Number of Vehicles	582,020	vehicles

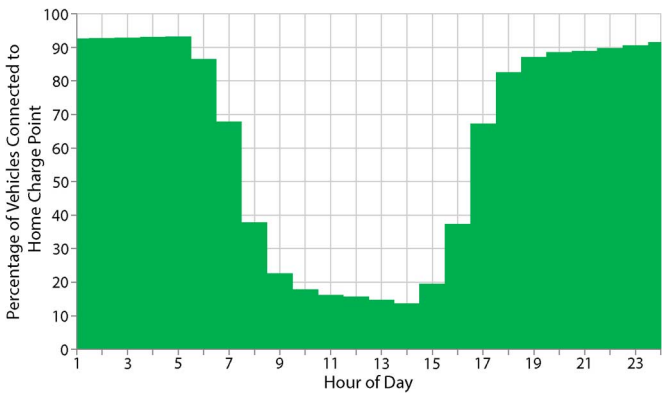

Fig. 9. Percentage of EVs that are connected to the power system at home charging points each day.

For simplicity, the state-of-charge of individual batteries is not considered. Instead it is assumed that the daily EV charging demand is equal to the daily average of the annual charging demand. Since the vehicles just replenish what they use, the state-of-charge of the batteries will not exceed capacity. Also, assuming a vehicle is fully charged to its maximum desired level on some date, replenishing the energy that was used will ensure that the battery returns to this state each day.

The rate of charging is constrained by a charging availability series, i.e. the percentage of vehicles that are connected to a charging point at each hour of the day (Fig. 9). The series is derived from US census data [22] which gives the percentage of respondents leaving for work during defined time-ranges. It is then assumed that on average, vehicles return 9 hours after their departure, corresponding roughly to an 8 hour working day plus twice the average commute time. This characterization of EV availability assumes every vehicle is a commuter vehicle and that there are no non-commuting trips. Each grid-connected vehicle is assumed to be able to charge at 3.3 kW, reflecting current level 2 charging capabilities [23]. It should be noted that there is a variety of EV charging standards and capabilities. Additionally, charging rates are constrained by the maximum ratings on the distribution networks to which the EVs are connected. Finally, there will be situations where the state-of-charge of a battery is too high to provide a full rate of charge for the period the vehicle is grid-connected. Thus the system charging availability series will be somewhat overstated. However, since vehicles will tend to be grid-connected for long periods, and thus average charging rates will tend to be quite low, it is unlikely that charging availability will significantly constrain vehicle charging. Given the average annual distance traveled by each vehicle (km/year), and an average vehicle efficiency (kWh/km), the number of vehicles can be determined (Table III). In combination with the charging availability series (in %), the maximum charging power at each hour can be determined. The charging availability series offers the greatest charging availability at hours where charging demand will tend to be at its highest.

TABLE IV
ELECTRIC VEHICLE IMPACT QUANTIFIED OVER FOLLOWING PARAMETER SET

Parameter	*Values considered*
Systems	ERCOT, Finland, Germany, Ireland, Sweden
Wind Penetrations	0, 10, 20, 30, 40, 50%
EV Penetrations	0, 5, 10, 15, 20, 25%
CO_2 Costs	0, 10, 20, 30, 40, 50, 60, 70, 80 €/t, CO_2
total = 1620 cases	

Electricity demand tends to be highest in the evenings and is at its lowest during the night. To reflect this, the 24-hour period over which vehicle charging is scheduled is offset by 6 hours, such that it starts and ends at 6 pm. This tends to place the nighttime demand minimum roughly in the centre of the charging period whilst aligning the start of the charging period with the mean home arrival time. All of the charging for a particular day must take place within this charging window.

The complete long-term impact of EVs is isolated by calculating the difference in costs, both fixed and variable, over a ten year period, between a scenario with a particular EV penetration and the same scenario with no EVs. This is presented as the average annual increase in system costs, per vehicle and will be referred to herein as the *Electric Vehicle Impact* (EVI). This metric has been quantified over an extensive set of parameters (Table IV).

IV. RESULTS

A. EVI in Base Configuration

First, EVI, which is equivalent to the net-cost to the power system of supplying the required EV charging energy, is presented for each system in its base configuration, i.e. with no wind installed, no CO_2 costs and a minimal EV penetration (0.5%) (Fig. 10). The left column in each pair gives EVI under the assumption of controlled charging, as described in Section II. The right column again presents EVI but where charging is uncontrolled. Here it is assumed that vehicles begin charging on home arrival (according to the commuter model described in Section III) at the maximum rate (3.3 kW) until the average daily vehicle energy use (11.4 kWh) has been replenished. This corresponds to 3.45 hours of charging for each vehicle. It can be seen that controlled charging yields substantial savings, but that the level of saving varies strongly between systems.

Moreover, the level of EV impact can be extremely sensitive to changes in any of the input parameters. With respect to the base configuration, as the number of EVs is increased at a high resolution (Fig. 11), step changes in EVI can be seen, which are a response to changes in the final set of generators arising from the capacity expansion. Thus the chosen EV penetration in the base configuration can have a dramatic effect on the base EVI.

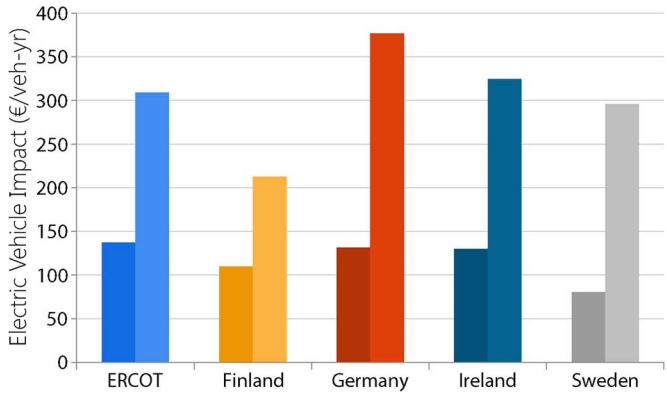

Fig. 10. Electric vehicle impact for controlled charging (left column in each pair) and uncontrolled charging (right column in each pair) in the base configuration (0.5% EVs, 0% wind penetration, euros 0 CO_2 cost).

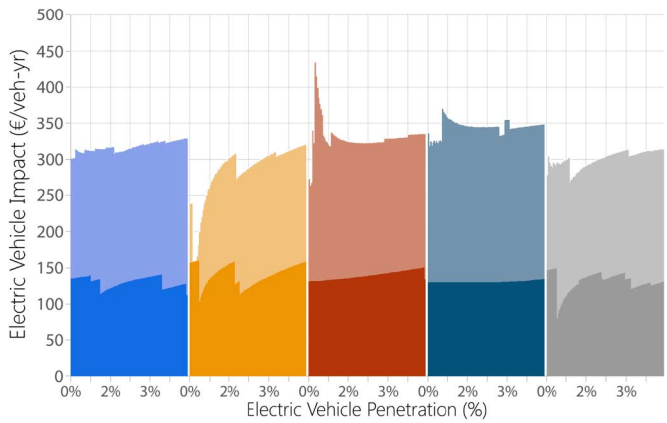

Fig. 11. EV impact as a function of increasing EVs for all demand series (0% wind penetration, euros 0 CO_2 cost, 0–5% EVs). The lighter plots represent the uncontrolled charging case. The dark plots to the front represent the controlled charging case.

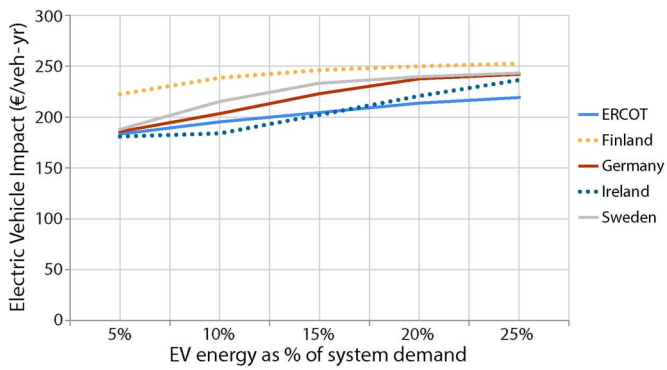

Fig. 12. Annual per-vehicle impact as a function of EV penetration for all systems (0% wind penetration, euros 30 CO_2 cost).

B. EVI Against EV Penetration

Next, it is shown (Fig. 12) how the impact of EVs is influenced by the EV penetration.

Initial increments of EV demand will tend to increase the daily net-demand floor the most owing to the triangular or "U-shaped" geometry of troughs, which increases in width towards the top (Fig. 13). Subsequent increments will increase it less but will also tend to increase the production from lower merit (higher unit cost) generation plant. As ever more increments are added, extra EV demand may even exacerbate peaks, forcing unit starts or even necessitating extra capacity where charging occurs at the annual peak. All of these effects mean that as EV demand increases on a system, the cost of meeting the extra demand will tend to increase also.

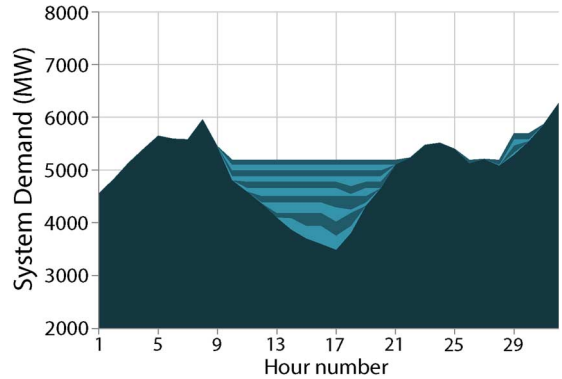

Fig. 13. Additions of equal increments of EV demand to a net-demand time-series (Ireland, 2008, 46% wind penetration) leading to successively smaller increases in minimum net-demand over the optimization horizon.

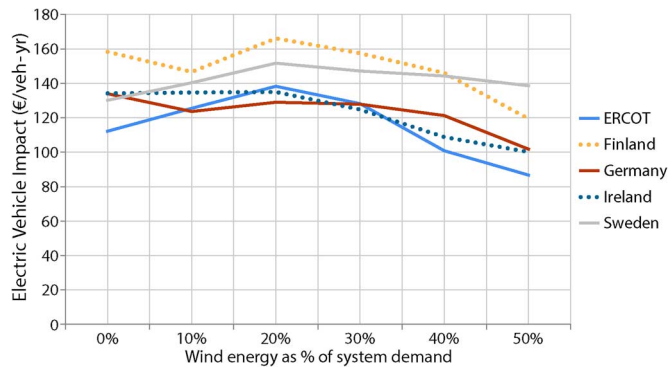

Fig. 14. Annual per-vehicle impact as a function of wind penetration for all systems (5% EV penetration, euros 0 CO_2 cost).

This is reflected in Fig. 12 where the impact of EVs increases for all systems as EV penetration increases. This relationship is generally replicated across the input set. The only exceptions are where an incremental increase in EV load leads to a large step-change in the optimal set of generation plant.

C. EVI Against Wind Penetration

The addition of wind plant can lead to more erratic changes in Electric Vehicle Impact (Fig. 14). At higher wind penetrations there is increased net-demand variability. Since EVs can reduce this variability, with an accompanying reduction in costs, EVI should be higher as wind levels increase. However, increases in variable generation also reduce the utilization of conventional generating units. The viability of high fixed cost generation relies on high capacity factors, however the most suitable plant types to take the place of high fixed cost units is not obvious. As an example (Fig. 15), when the capacity of coal falls in the final optimal plant mix, there is an increase in CCGT generation while there are oscillations in ADGT and CCGT capacity.

At higher CO_2 cost levels, a more stable dynamic is seen (Fig. 16). Higher CO_2 costs relatively affect coal investment to the greatest extent and in this case there are no coal units

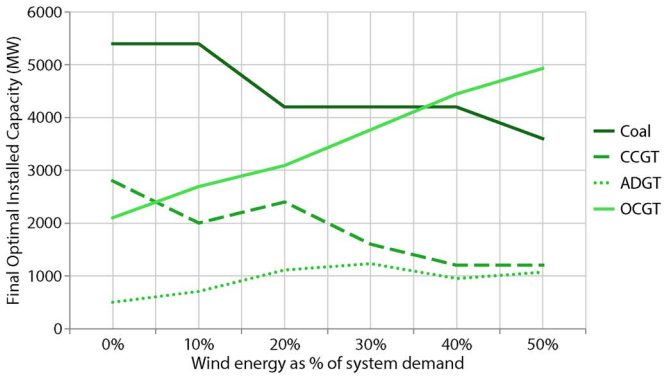

Fig. 15. Final levels of installed plant for increasing levels of installed wind (Sweden, 5% EV penetration, euros 0 CO_2 cost).

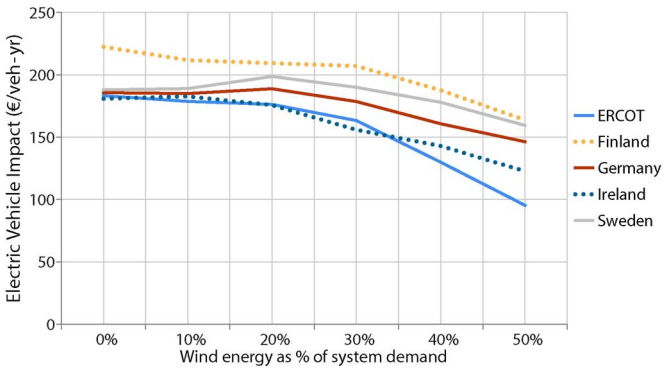

Fig. 16. Annual per-vehicle impact as a function of wind penetration for all systems (5% EV penetration, euros 30 CO_2 cost).

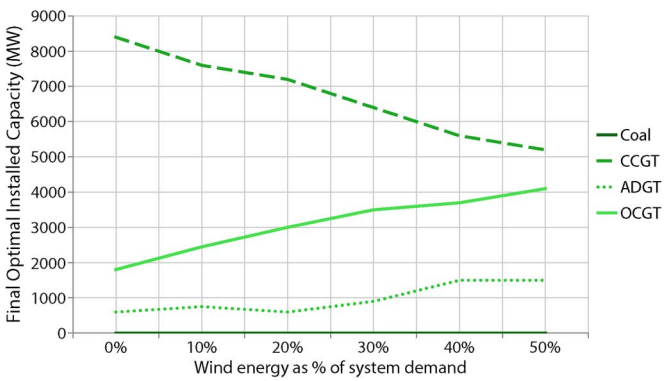

Fig. 17. Final levels of installed plant for increasing levels of installed wind (Sweden, 5% EV penetration, euros 30 CO_2 cost).

in the final plant mix. Since the installed capacity of only one inflexible generation type (i.e. CCGT) increases, changes in EV impact are more consistent and accord to expectations. The changes in the optimal set of generators (Fig. 17), whilst large, are stable across the range of wind penetrations.

D. EVI Against CO_2 Cost

The greatest level of volatility in Electric Vehicle Impact occurs where the relative price of coal and gas is such that changes in either price will lead to large changes in the optimal capacity of generation from the fuels. Changes in the relative price of the fuels can be represented by varying the cost of CO_2 permits, since the cost of CO_2 relatively affects the price of coal

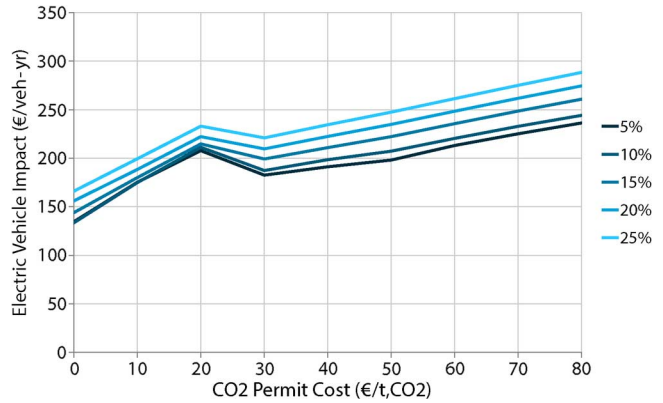

Fig. 18. Annual per-vehicle impact as a function of CO_2 cost for all EV penetrations (Ireland, 10% wind penetration).

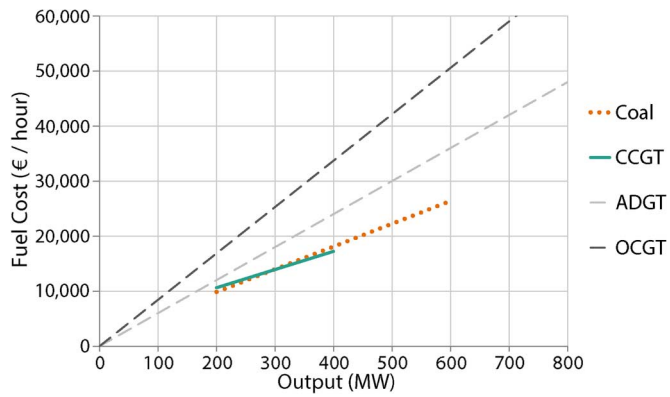

Fig. 19. Hourly costs (sum of no-load and incremental costs) as a function of generator electrical output for each generation type $(\text{euros } 20/t, CO_2)$.

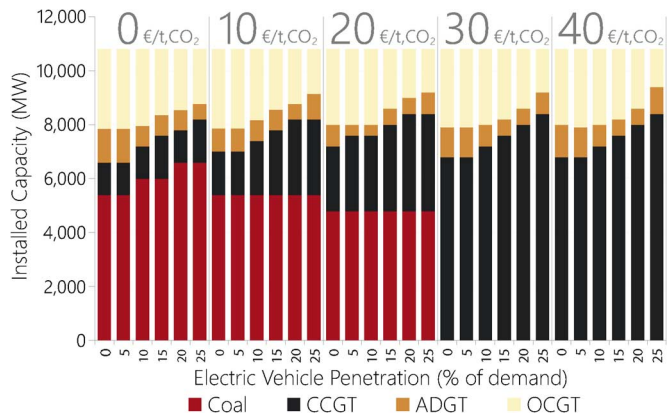

Fig. 20. Final installed capacities for selected CO_2 cost levels and electric vehicle penetrations (Ireland, 10% wind).

more than the price of gas (coal releases more CO_2 per unit of energy than natural gas).

Fig. 18 presents EVI as a function of CO_2 cost. A large spike in vehicle impact occurs in the region of 20–30 euros/t, CO_2. At 20 euros/t, CO_2, CCGT generation begins to offer lower cost power than coal at high output levels (Fig. 19). Nevertheless, the coal units have lower start costs (Table II) and since they are competitive at low output levels, they still appear in the least-cost set of generators (Fig. 20). However, at 30 euros/t, CO_2, coal generation is much more costly than production from

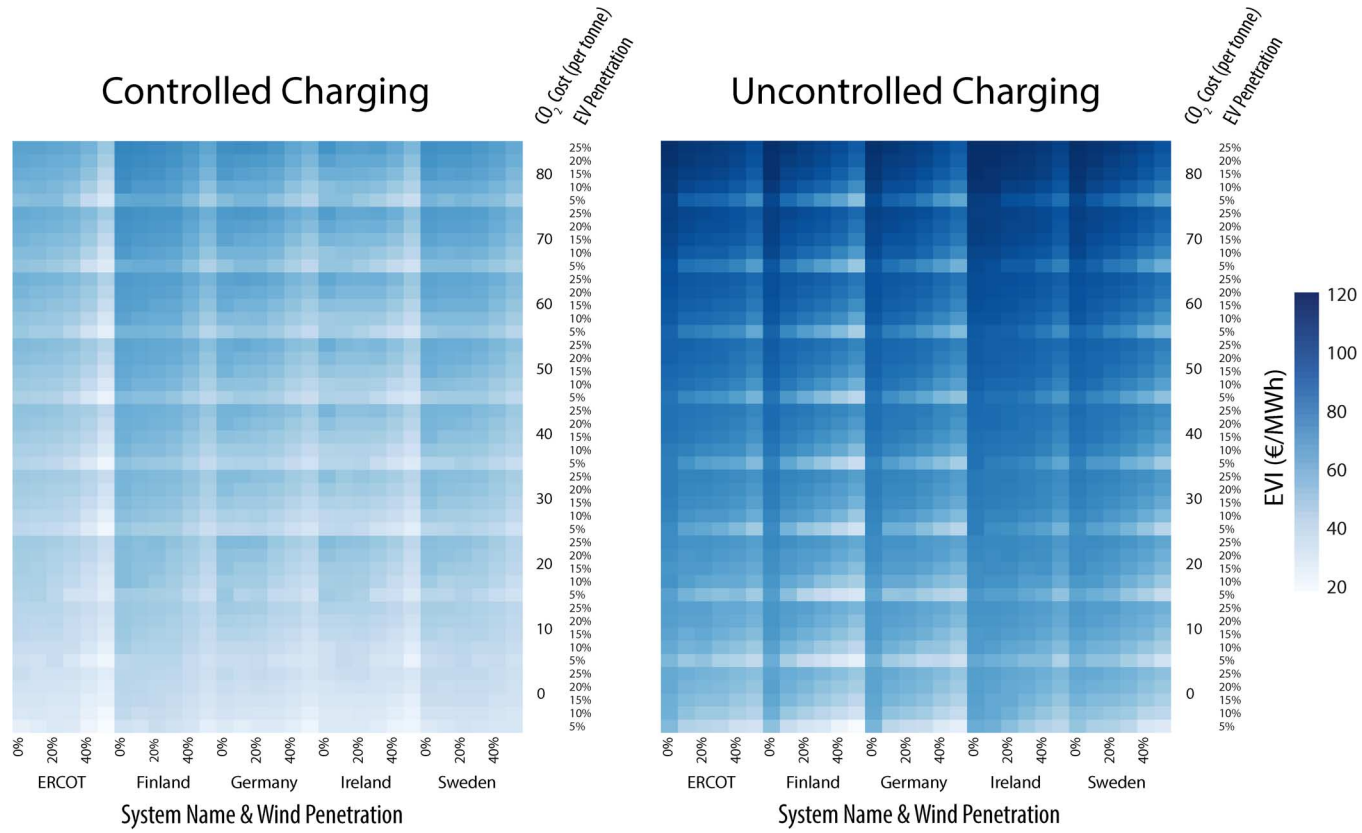

Fig. 21. Electric vehicle impact for optimal and uncontrolled charging cases.

CCGT units and thus no longer appears at all in the final generation mix (Fig. 20).

The step-changes in EVI between 20 and 30 euros/t, CO_2 occur because much of the EV demand will be met by generation that would have been online in the absence of any EVs. Incremental costs are a much smaller fraction of full-load costs for CCGT plants than for coal plants, thus EVI is often lower in high net-demand variability cases where CCGT is the dominant baseload technology.

The final result returns to the comparison made at the start of the section between controlled and uncontrolled charging. Since full user participation in direct or indirect charging control may not be feasible, this provides a worst-case scenario in that respect. The average EVI (presented here in units of euros/MWh) for the controlled charging case is 51.5 euros/MWh (ranging from 20.8 to 77.5 euros/MWh). For the uncontrolled case, the average is far higher, averaging 94.1 euros/MWh and ranging from 45.7 to 120.4 euros/MWh). This indicates that there may be a sufficient incentive for system operators to establish some level of direct or indirect control over EV charging.

V. Conclusions

This paper has sought to determine the cost of electric vehicle charging, once the potential mutual benefits between the vehicles and the power generation fleet have been taken into account. When charged in a manner that is optimal to the power system, EVs can increase generator capacity factors and reduce costly baseload starts and part-loading. In the long-term, this will encourage increased investment in higher efficiency plants, which may be more costly to cycle and require higher levels of utilization to justify their installed cost.

The net-cost of EV charging, termed the *Electric Vehicle Impact*, is found to vary significantly across a number of parameters. First, the particular characteristics of demand variability are important: greater seasonality leads to increased charging by peaking generation, reducing EV benefit, whilst increased diurnality increases baseload cycling, which provides the opportunity for EVs to reduce costs. Second, Greater numbers of EVs will tend to lead to diminishing returns from EVs, owing partly to the inherent geometry of demand troughs but also since additional increments of charging use successively lower-merit generation. Third, increased wind penetration will tend to increase EV benefit, but can also incentivize the provision of more flexible generation, which has less to gain from EVs and tends to cost the system more. Finally, the relative level of fuel costs, which is affected by the cost of CO_2 emissions, can dictate very large changes in the installed set of generators over time, which will favor EVs where the changes would lead to increases in cycling costs.

The need for unit-commitment and the breadth of scenarios studied meant that a conventional methodology would be computationally impractical. A new unit-commitment algorithm has therefore been developed for this purpose. A methodology such as this could be used to inform the design of tariffs for electric vehicle charging, returning some of the potential benefits of optimized charging to the vehicle user.

VI. Future Work

Specific systems present specific challenges and allow for the opportunity to consider an expanded range of generation and ancillary technologies. For example, solar power presents very different statistical properties to wind. This may require data at higher resolutions and different modeling approaches. Each system presents unique constraints and topologies at the transmission and distribution levels. Thus, the charging regimes here can be contrasted to charging strategies that are optimal with respect to particular network configurations.

EVs are one of many sources of power system flexibility. Ideally these should all be considered together, in particular where flexibility may be the primary purpose of a particular investment, e.g. pumped storage or HVDC lines.

An attractive feature of EVs is the elimination of point-of-use emissions. Additional system demand will lead to an increase in emissions of CO_2 and changes in levels of other pollutants, and so the net-emissions in each emissions category should be calculated. This could build upon the work of [16].

There are certain assumptions that have been made in this analysis which could be investigated in more depth. For example, using higher resolution wind and demand time-series may lead to increased cycling costs, reducing EV impact further.

Finally, least-cost investment has been assumed here, but there are many reasons why actual investment will differ. Thus the impact of EVs under different market and regulatory arrangements would be worth pursuing.

Appendix A
Performance of FAST Algorithm

The FAST algorithm can be compared to its equivalent MIP formulation in terms of the *optimality* of the schedules (the degree to which cost are minimized), the *similarity* of the schedules and finally, the computation time. First, the formulation of the equivalent is given.

A. Equivalent MIP Formulation

The objective function (3) is the sum of hourly production costs for the whole year.

$$f_{obj} = \sum_{t \in T} G(t) \tag{3}$$

The hourly costs (4) equal the costs from the inflexible types (start, no-load and incremental costs) added to the costs for the flexible types (average costs).

$$\begin{aligned} G(t) = \sum_{U_{in}} & \left(C_{start}(u_{in}) \cdot V_{start}(u_{in}, t) + C_{NL}(u_{in}) \right. \\ & \left. \cdot V_{online}(u_{in}, t) + C_{incr}(u_{in}) \cdot V_{gen}(u_{in}, t)\right) \\ & + \sum_{U_{fl}} \left(C_{avg}(u_{fl}) \cdot V_{gen}(u_{fl}, t)\right) \forall t \end{aligned} \tag{4}$$

The sum of production from inflexible, flexible and wind generation (less curtailment) must equal the electricity demand for each hour (5).

$$\sum_{U_{all}} V_{gen}(u_{all}, t) + P_{wind}(t) - V_{curt}(t) = P_{dem}(t) \forall t \tag{5}$$

Wind curtailment (6) must be less than or equal to wind production in each hour.

$$V_{curt}(t) \leq P_{wind}(t) \forall t \tag{6}$$

The sum of online inflexible capacity less the sum of inflexible production (i.e. the quantity of spinning reserve) must exceed a pre-defined target (7). For simplicity, here this target is set to the size of the largest installed unit, where at least one such unit exists.

$$P_{res} \leq \sum_{U_{in}} \left(V_{online}(u_{in}, t) \cdot P_{max}(u_{in})\right) - \sum_{U_{in}} \left(V_{gen}(u_{in}, t)\right) \forall t \tag{7}$$

Production from any type cannot exceed the quantity installed. Similarly, the number of online inflexible units cannot exceed the number installed (8).

$$V_{gen}(u_{all}, t) \leq I(u_{all}) \forall t, u_{all} \tag{8}$$

$$V_{online}(u_{in}, t) \leq N(u_{in}) \forall t, u_{in} \tag{9}$$

Production from any inflexible type is bounded by minimum (10) and maximum (11) output levels and the number of online units of that type.

$$V_{gen}(u_{in}, t) \geq V_{online}(u_{in}, t) \cdot P_{min}(u_{in}) \forall t, u_{in} \tag{10}$$

$$V_{gen}(u_{in}, t) \leq V_{online}(u_{in}, t) \cdot P_{max}(u_{in}) \forall t, u_{in} \tag{11}$$

Finally, the number of starts for an inflexible type (V_{start}) is set to the increase in the number of online units (V_{online}) for that type (12).

$$V_{start}(u_{in}, t) \geq V_{online}(u_{in}, t) - V_{online}(u_{in}, t-1) \forall t, u_{in} \tag{12}$$

B. Performance Comparison

The FAST algorithm and its equivalent MIP is compared across a broad range of input parameters. For 3 plant types (coal, CCGT, OCGT), all combinations of plant equalling 11.8 GW installed capacity (271) are considered on the 5 systems-ERCOT, Finland, Germany, Ireland, Sweden—where each demand-series is scaled to 10 GW peak. 6 levels of installed wind (0 GW to 10 GW in steps of 2 GW) and a cost-set reflecting recent European fuel spot prices is used [27].

1) Optimality: A MIP is usually not solved to optimality. Instead, once a set of decision variable values is found such that the objective function value of the MIP is within some tolerance of the objective function value of the the solution of the relaxed form of the MIP, the solution is accepted as *integer optimal*. This tolerance is called the optimality gap. An equivalent optimality gap can be calculated for schedules from the FAST algorithm to compare the optimality of the methods. In order to focus on the important plant combinations, for each system and wind level, the optimality gap for both methods is given for the ten lowest total costs plant combinations (Fig. 22).

2) Similarity: To compare the similarity of the unit-commitments from the two methods, the total online inflexible capacity for the ten lowest total cost plant combinations is presented in Fig. 23 for each system and wind combination.

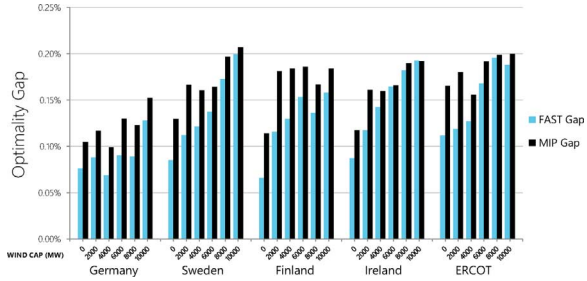

Fig. 22. Optimality gap for FAST and equivalent MIP, averaged over the ten generation plant combinations with lowest total costs.

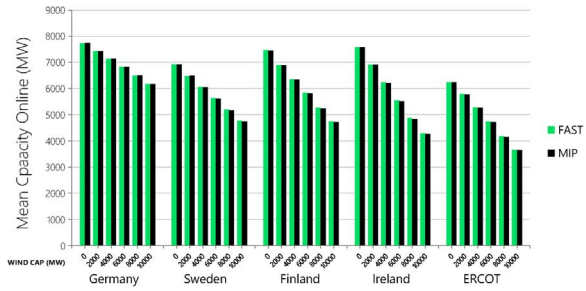

Fig. 23. Mean combined CCGT and coal online capacity for FAST and equivalent MIP, averaged over the ten plant combinations with lowest total costs.

TABLE V
COMPUTATION TIME STATISTICS FOR THE MIP AND THE *FAST* ALGORITHM

Model	*Metric*	*Time*	*Unit*
MIP	Max	636	*s*
	Min	7	*s*
	Mean	27	*s*
	Median	22	*s*
FAST	Mean	20	*ms*

3) Computation Time: Finally, the computation time is compared for all of the plant combinations considered (Table V). It is seen that the computation time for the equivalent MIP is over a thousand times longer than for the FAST algorithm.

The much reduced computation time for the algorithm is achieved by utilizing a logical structure that requires the consideration of only a relatively small number of potential commitments, i.e. those that could potentially reduce costs. An example of this is the use of the relative magnitude of net-capacity demand and online inflexible capacity as a criterion for considering changes in the commitment (Fig. 2).

APPENDIX B
PORTFOLIO TRAJECTORY EXAMPLE

Given the number of cases considered, it is not possible to present the generation portfolio trajectory for each case. Nevertheless, an example of how the portfolio adapts to the addition of EVs is given to provide insight into this process. The chosen case, which appears in the text of Section IV-D and to varying degrees in Figs. 18–20, represents the *Ireland*, 10% wind penetration, 25% EV penetration and 20 euros/t CO_2 tax case.

It is seen (Fig. 24) that the large-scale introduction of EVs reduces the need for coal's part-loading performance and enables the introduction of CCGT generation, which for this CO_2 cost level offers the lowest production costs at higher loading levels (see Fig. 19).

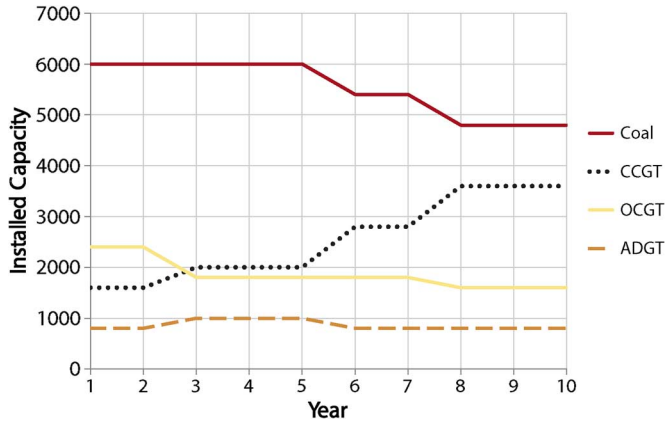

Fig. 24. Installed capacity of each generation type for each year of the study period (Ireland, 10% wind, 25% EVs, euros $20/t, CO_2$).

TABLE VI
YEAR OF RETIREMENT FOR EACH INFLEXIBLE UNIT. A RETIREMENT YEAR IS PROVIDED FOR EACH UNIT UP TO A MAXIMUM OF 16 INSTALLED UNITS OF EITHER TYPE

Type	Unit Number							
	1	2	3	4	5	6	7	8
Coal	0	5	0	7	1	6	4	9
CCGT	1	6	4	9	1	5	2	5
Type	Unit Number $(cont'd)$)							
	9	10	11	12	13	14	15	16
Coal	0	5	2	7	1	6	4	9
CCGT	1	5	4	9	0	5	2	7

TABLE VII
YEARS AT WHICH BLOCKS OF CAPACITY OF EACH TYPE ARE RETIRED

Type	Block Number	
	1	2
OCGT	0	5
ADGT	2	7

APPENDIX C
RETIREMENT SCHEDULES

Generation capacity is retired according to pre-defined retirement schedules. This is done so that capacity retirements do not vary across the studied cases. It is assumed that the capacity expansion duration (10 years) divided by the life of the plant in question (30 years for coal, 20 years for the CCGT, ADGT and OCGT) gives the fraction of capacity of that type that will be retired over the period. Thus, 1/2 of the initial CCGT, OCGT and ADGT capacity will retire and 1/3 of the coal capacity will retire over the 10 year capacity expansion period. When an expansion in capacity is required, the candidate options will be considered for the life of the longest plant under consideration, which is usually 30 years. Retirements that would occur over that period are not considered at that point though, since that would require expansions within expansions. Since the initial capacity of each plant type varies based on the demand and wind series used, each unit is numbered and has a year that it will retire in, if it is installed (see Table VI). For example, if there are 6 coal plants in the initial portfolio, 2 will retire. The first will retire in year zero and the second in year 5.

The flexible types are retired in two blocks (Table VII). The purpose of doing this is to have certain years where larger

amounts of capacity retires, which reduces the impact of the integral nature of unit expansions. For example, where there is a 400 MW deficit, a 400 MW CCGT plant will have a significant advantage over a 600 MW coal unit.

REFERENCES

[1] "Environmental Assessment of Plug-In Hybrid Electric Vehicles," Electric Power Research Institute, Tech. Rep., Palo Alto, CA, USA, 2007.

[2] U. Bossel, "The hydrogen illusion: Why electrons are a better energy carrier," *Cogeneration and On-Site Power Production*, pp. 55–59, 2004.

[3] K. Parks, P. Denholm, and A. J. Markel, "Costs and Emissions Associated With Plug-In Hybrid Electric Vehicle Charging in the Xcel Energy Colorado Service Territory,: National Renewable Energy Laboratory (NREL), Tech. Rep., 2007.

[4] P. Denholm and W. Short, "Evaluation of Utility System Impacts and Benefits of Optimally Dispatched Plug-In Hybrid Electric Vehicles (Revised)," National Renewable Energy Laboratory (NREL), Tech. Rep., 2006.

[5] J. P. Lopes, F. J. Soares, and P. R. Almeida, "Integration of electric vehicles in the electric power system," *Proc. IEEE*, vol. 99, no. 1, pp. 168–183, 2011.

[6] "Damage to Power Plants Due to Cycling," Electric Power Research Institute, Tech. Rep., Palo Alto, CA, USA, 2001.

[7] "Correlating Cycle Duty With Cost at Fossil Fuel Power Plants," Electric Power Research Institute, Tech. Rep., Palo Alto, CA, USA, 2001, Tech. Rep..

[8] N. Troy, E. Denny, and M. O'Malley, "Base-load cycling on a system with significant wind penetration," *IEEE Trans. Power Syst.*, vol. 25, no. 2, pp. 1088–1097, 2010.

[9] *Commercial Offer Data—Standard Generator* Single Electricity Market Operator, Ireland, Last accessed November 2012 [Online]. Available: http://www.sem-o.com/marketdata/Pages/PricingAndScheduling.aspx

[10] A. Shortt and M. O'Malley, "Impact of optimal charging of electric vehicles on future generation portfolios," in *Proc. Conf. Sustainable Alternative Energy (SAE), 2009 IEEE PES/IAS*, Sep. 2009, pp. 1–6.

[11] W. Short and P. Denholm, "Preliminary Assessment of Plug-In Hybrid Electric Vehicles on Wind Energy Markets," National Renewable Energy Laboratory (NREL), Tech. Rep., Golden, CO, USA, 2006.

[12] P. Denholm and W. Short, "Evaluation of Utility System Impacts and Benefits of Optimally Dispatched Plug-In Hybrid Electric Vehicles (Revised)," National Renewable Energy Laboratory (NREL), Tech. Rep., Golden, CO, USA, 2006.

[13] J. Kiviluoma and P. Meibom, "Influence of wind power, plug-in electric vehicles, and heat storages on power system investments," *Energy*, vol. 35, no. 3, pp. 1244–1255, 2010.

[14] A. Shortt, J. Kiviluoma, and M. O'Malley, "Accommodating variability in generation planning," *IEEE Trans. Power Syst.*, vol. 28, no. 1, pp. 158–169, Feb. 2013.

[15] CPLEX 12, Section: Mixed-Integer Programming IBM ILOG [Online]. Available: http://www.gams.com/dd/docs/solvers/cplex.pdf

[16] R. Sioshansi and P. Denholm, "Emissions impacts and benefits of plug-in hybrid electric vehicles and vehicle-to-grid services," *Environ. Sci. Technol.* vol. 43, no. 4, pp. 1199–1204, 2009 [Online]. Available: http://pubs.acs.org/doi/abs/10.1021/es802324j

[17] C. Gellings, "The concept of demand-side management for electric utilities," *Proc. IEEE*, vol. 73, no. 10, pp. 1468–1470, 1985.

[18] "Cost and Performance for Power Generation Technologies," Prepared for the National Renewable Energy Laboratory by Black & Veatch, (Feb. 2013) [Online]. Available: http://bv.com/docs/reports-studies/nrel-cost-report.pdf

[19] Generator Data Parameters "All Island Project,", (Nov. 2012) [Online]. Available: http://www.allislandproject.org/zip/Datasheets%20Public.zip

[20] W. Katzenstein, E. Fertig, and J. Apt, "The variability of interconnected wind plants," *Energy Policy*, vol. 38, no. 8, pp. 4400–4410, 2010.

[21] Monthly World Prices of Commodities and Indices World Bank, (Aug. 2012) [Online]. Available: http://siteresources.worldbank.org/INTPROSPECTS/Resources/334934-1304428586133/PINK_DATA.xlsx

[22] Journey to Work: (Census 2000 Brief) United States Census Bureau, USA, (Jul. 2011) [Online]. Available: http://www.census.gov/prod/2004pubs/c2kbr-33.pdf

[23] M. Yilmaz and P. Krein, "Review of battery charger topologies, charging power levels, and infrastructure for plug-in electric and hybrid vehicles," *IEEE Trans. Power Electron.*, vol. 28, no. 5, pp. 2151–2169, May 2013.

[24] Office of Highway Policy Information-Highway Statistics Series Federal Highway Administration, USA, (Aug. 2012) [Online]. Available: http://www.fhwa.dot.gov/policyinformation/statistics/abstracts/tx.cfm

[25] Nissan Leaf Specifications Nissan, (Aug. 2012) [Online]. Available: http://www.nissan.ie/vehicles/leaf/

[26] Mitsubishi i-MiEV Specifications Mitsubishi Motors, (Aug. 2012) [Online]. Available: http://i.mitsubishicars.com/miev/features/compare/

[27] Natural Gas Spot & Coal Futures Prices European Energy Exchange, (Dec. 2010) [Online]. Available: http://www.eex.com/

Aonghus Shortt (S'09) received the B.E. degree from University College Dublin, Dublin, Ireland, in 2008, where he is currently pursuing the Ph.D. degree with research interests in electric vehicles, wind power generation and power system planning and investment.

Mark O'Malley (F'07) received the B.E. and Ph.D. degrees from University College Dublin, Dublin, Ireland, in 1983 and 1987, respectively.

He is currently Professor of Electrical Engineering at University College Dublin and director of the Electricity Research Centre with research interest in power systems, control theory, and biomedical engineering.